



Research papers

Influences of recent climate change and human activities on water storage variations in Central Asia

Haijun Deng^{a,b}, Yaning Chen^{a,*}^aState Key Laboratory of Desert and Oasis Ecology, Xinjiang Institute of Ecology and Geography, Chinese Academy of Sciences, Urumqi 830011, China^bUniversity of Chinese Academy of Sciences, Beijing 10049, China

ARTICLE INFO

Article history:

Received 4 August 2016

Received in revised form 2 November 2016

Accepted 4 November 2016

Available online 5 November 2016

This manuscript was handled by Tim R.

McVicar, Editor-in-Chief, with the assistance of Di Long, Associate Editor

Keywords:

Terrestrial water storage

Climate change

Human activities

GRACE

Central Asia

ABSTRACT

Terrestrial water storage (TWS) change is an indicator of climate change. Therefore, it is helpful to understand how climate change impacts water systems. In this study, the influence of climate change on TWS in Central Asia over the past decade was analyzed using the Gravity Recovery and Climate Experiment satellites and Climatic Research Unit datasets. Results indicate that TWS experienced a decreasing trend in Central Asia from 2003 to 2013 at a rate of -4.44 ± 2.2 mm/a, and that the maximum positive anomaly for TWS (46 mm) occurred in July 2005, while the minimum negative anomaly (-32.5 mm) occurred in March 2008–August 2009. The decreasing trend of TWS in northern Central Asia (-3.86 ± 0.63 mm/a) is mainly attributed to soil moisture storage depletion, which is driven primarily by the increase in evapotranspiration. In the mountainous regions, climate change exerted an influence on TWS by affecting glaciers and snow cover change. However, human activities are now the dominant factor driving the decline of TWS in the Aral Sea region and the northern Tarim River Basin.

© 2016 Elsevier B.V. All rights reserved.

1. Introduction

Terrestrial water storage (TWS) comprises groundwater, soil moisture, surface water bodies (lakes, rivers, and reservoirs), glaciers, snow water equivalent, and canopy water storage (Syed et al., 2008; Tangdamrongsub et al., 2015). TWS can be described by the water balance equation $\Delta W = P - R - E$, where ΔW is terrestrial water storage, P is precipitation, R is runoff, and E is evapotranspiration. Changes in temperature and wind speed cause variations in evapotranspiration, which, in turn, cause changes in TWS. TWS is a transient state that is dependent on the relationship between the input (i.e., precipitation and runoff) and output (i.e., evapotranspiration, runoff, and human water use). Global water storage is balanced because input and output are essentially equal on a global scale. However, there are differences between input and output across different regions and seasons, with variations in TWS exhibiting seasonal characteristics (Hirschi et al., 2006; Grippa et al., 2011; Yang and Chen, 2015).

Because TWS is a key variable in the hydrological cycle (Hirschi et al., 2006), it has significant ecological, environmental, societal, and economic impacts (Ramillien et al., 2005; Long et al., 2014;

Cao et al., 2015). Glacier and snow melt are important water resources in semi-arid and arid regions, especially in Central Asia (Sorg et al., 2012; Chen et al., 2015), and are affected by various effects of climate change on TWS (Immerzeel et al., 2010; Sorg et al., 2012). Glaciers and snow are important components of TWS in mountainous areas (Aizen et al., 1997), including the study area where most of the rivers originate from the Tian Shan Mountains. Recent research results indicate that increases in glacier and snow melt decreased TWS in the mountain regions (Matsuo and Heki, 2010) but increased it in the surrounding basin area (Yang et al., 2015).

Since being launched in March 2002, the Gravity Recovery and Climate Experiment (GRACE) mission has provided data that can be used for analyzing TWS. Examples of areas that have been studied using GRACE data include the Congo Basin (Crowley et al., 2006), the Mississippi River Basin (Zaitchik et al., 2008), the Amazon Basin (Xavier et al., 2010), and the Yangtze River Basin (Long et al., 2015). Table 1 presents a summary of the relevant literature on estimated TWS variations based on GRACE datasets.

Investigations indicate that climate change has intensified water resources stress in Central Asia over the past few decades. Temperatures have exhibited a rising trend, and precipitation variability has increased (Lioubimtseva et al., 2005; Mannig et al., 2013; Li et al., 2015). Climate change has also led to increasing river runoff variability (Bernauer and Siegfried, 2012) and is

* Corresponding author at: Xinjiang Institute of Ecology and Geography, Chinese Academy of Sciences, No. 818 South Beijing Road, Urumqi 830011, China.

E-mail address: chenyn@ms.xjbg.ac.cn (Y. Chen).

Table 1

Summary of relevant literature on terrestrial water storage based on GRACE datasets in relation to the aims of this study, which are: (1) to analyze TWS variations; (2) to determine applications of TWS to groundwater, evapotranspiration, flood and drought, and glaciers mass balance; and (3) to analyze the effects of climate change and human activities on TWS variations. We added the current study for completeness. Studies are first listed chronologically, and then in alphabetical order. The symbol 'n.r.' means 'not reported'.

Study	Scales	Degree/spatial resolution/time span	Key results
1-Ramillien et al. (2005)	Global	30/660 km/2 years	1. Estimate water volume changes over eight large river basins in the tropics 2. Estimate an average value of the evapotranspiration over each river basin, using the water balance equation 3. n.r.
2-Crowley et al. (2006)	Congon Basin	70/600 km/4 years	1. Estimates exhibit significant seasonal (30 ± 6 mm of equivalent water thickness) and long-term trends 2. n.r. 3. Precipitation contributed roughly three times the peak water storage after anomalously rainy seasons, in early 2003 and 2005
3-Strassberg et al. (2014)	USA	n.r./400 km/30 months	1. Correlation between GRACE-based TWS and measured GWS is significant ($R = 0.58$) 2. The results show the potential for GRACE to monitor groundwater storage changes in semiarid regions 3. n.r.
4-Yirdaw et al. (2008)	Canadian Prairie	n.r./800 km/46 months	1.The TWS decreased over the whole of Western Canada 2.Drought assessment 3.n.r.
5-Rodell et al. (2009)	Northwest India	60/300 km/73 months	1. n.r. 2. During the period of August 2002 to October 2008, groundwater depletion was equivalent to a net loss of 109 km^3 of water 3.Caused by irrigation and other anthropogenic uses
6-Xavier et al. (2010)	Amazon Basin	n.r./300 km/73 months	1. Focused on interannual variability of TWS over 2003–2008 2. n.r. 3. TWS shown to be highly correlated with the ENSO
7-Grippa et al. (2011)	West Africa	60/400 km/2003–2007 years	1. Water storage spatial distribution, including zonal transects, its seasonal cycle, and its interannual variability 2. n.r. 3. n.r.
8-Houborg et al. (2012)	America	60/300 km/August 2002 to July 2009	1.n.r. 2. GRACE-based drought indicators 3. n.r.
9-Feng et al. (2013)	North China	60/200/2003–2010	1. n.r.; 2. The rate of groundwater depletion in North China was 2.2 ± 0.3 cm/a from 2003 to 2010 3. Caused by Irrigation
10-Long et al. (2013)	Texas	n.r./n.r./one year	1. GRACE shows depletion in TWS of $62.3 \pm 17.7 \text{ km}^3$ during the 2011 drought 2. Drought detect 3. n.r.
11-Thomas et al. (2014)	Amazon, Zambezi, Texas, southeastern United states	n.r./n.r./127 months	1. n.r. 2. Combine storage deficits with event duration to calculate drought severity 3. n.r.
12-Long et al. (2015)	Global	60/300 km/January 2003–July 2013	1. Large differences in TWS anomalies from three processing approaches (scaling factor, additive, and multiplicative corrections) were found in arid and semiarid region, areas with intensive irrigation, and relatively small basins 2. n.r. 3. n.r.
13-Yi and Wen (2016)	United States	60/500 km/2003–2012	1. The equivalent water thickness increasing from -4 to 9.4 cm in the north and decreasing from 4.1 to -6.7 cm in the south 2. Drought assessment 3. n.r.
14-This study	Central Asia	60/300 km/2003–2013	1. (a) During the past decade, TWS variations in Central Asia presented a decreasing trend at a rate of -4.44 ± 2.2 mm/a; (b) The declining rate of TWS in western and northern Central Asia, Tian Shan Mountains, and northern Tarim River Basin are -10.68 mm/a, -3.86 mm/a, -3.6 mm/a, and -0.82 mm/a, respectively 2. n.r. 3. TWS decreased in northern Central Asia and Tian Shan Mountains was driven by climate factors, but in western Central Asia and northern Tarim River Basin was driven by human activities

driving more drought events (Lioubimtseva and Henebry, 2009). These effects will result in increased water resources stress (Siegfried et al., 2012) and consequently increase international conflicts over water resources in Central Asia (Bernauer and Siegfried, 2012).

As a semi-arid and arid region, Central Asia is highly vulnerable to changes in climate (Lioubimtseva and Henebry, 2009; Chen et al., 2016). Therefore, variations in TWS have significant impacts on the social and ecological environments of the region. However, previous studies paid little attention to the impact of climate

change on regional TWS changes in Central Asia. Therefore, in this study, our two main objectives are to: (1) characterize the variations of TWS in Central Asia; and (2) analyze the impacts of climate change and human activities on TWS. This paper is organized as follows: Section 2 presents the study area, data collection, and methods used in this study. Section 3 focuses on the results of TWS trends and the impacts of recent climate change and human activities on them. Sections 4 and 5 present the Discussion and Conclusions sections, respectively.

2. Data and methods

2.1. Study area

Central Asia covers about $566 \times 10^4 \text{ km}^2$ and is largely confined within $34^\circ 20' - 55^\circ 30' \text{ N}$ and $46^\circ 30' - 96^\circ 30' \text{ E}$ (Fig. 1). It contains five countries of the former Soviet Union (Kazakhstan, Tadjikistan, Kyrgyzstan, Uzbekistan, and Turkmenistan) as well as Xinjiang, an autonomous region in northwest China. There are several large water bodies distributed throughout this region, including the Caspian Sea ($37 \times 10^4 \text{ km}^2$), the Aral Sea ($1.716 \times 10^4 \text{ km}^2$ in 2004), Balkhash Lake ($1.716 \times 10^4 \text{ km}^2$), Issyk-Kul Lake ($0.6236 \times 10^4 \text{ km}^2$), and Bosten Lake ($0.1 \times 10^4 \text{ km}^2$). The Caspian Sea, which is located in western Central Asia, has the lowest elevation (as defined by McVicar and Körner, 2013) in the region, with a

mean water level of -26.5 m (<http://www.LEGOS.obs-mip.fr/soa/hydrologie/HYDROWEB>). Rivers in Central Asia mostly form internal drainage systems (e.g., the Syr Darya and Amu Darya), but some, like the Irtysh, are outflow rivers that drain towards larger water bodies such as the Arctic Ocean.

Given its mid-continental location, Central Asia is characterized by a typical continental climate. The area is situated far from oceans, so ocean water vapor rarely reaches this region. The water vapor transport system is mainly controlled by westerly circulation (Qi and Kulmatov, 2008). From 1901 to 2013, the annual mean temperature of Central Asia was $6.65 \text{ }^\circ\text{C}$ and the annual mean precipitation was 211 mm . The vegetation is mainly grassland (Fig. 1).

2.2. Data collection

2.2.1. GRACE data

The GRACE mission consists of two satellites that fly nominally 220 km apart in a polar orbit 500 km above Earth (available at <http://www.csr.utexas.edu/grace/>). GRACE provides monthly, weekly, and daily read-outs of the Earth's gravity field; The surface mass change data for land grid cells is available at the Jet Propulsion Laboratory (JPL) website (<http://grace.jpl.nasa.gov/>). The datasets are gridded at 1 by 1 degrees (Swenson, 2012). In this study, the variability of TWS in Central Asia was analyzed using monthly datasets of the gravity field time-series obtained from GRACE

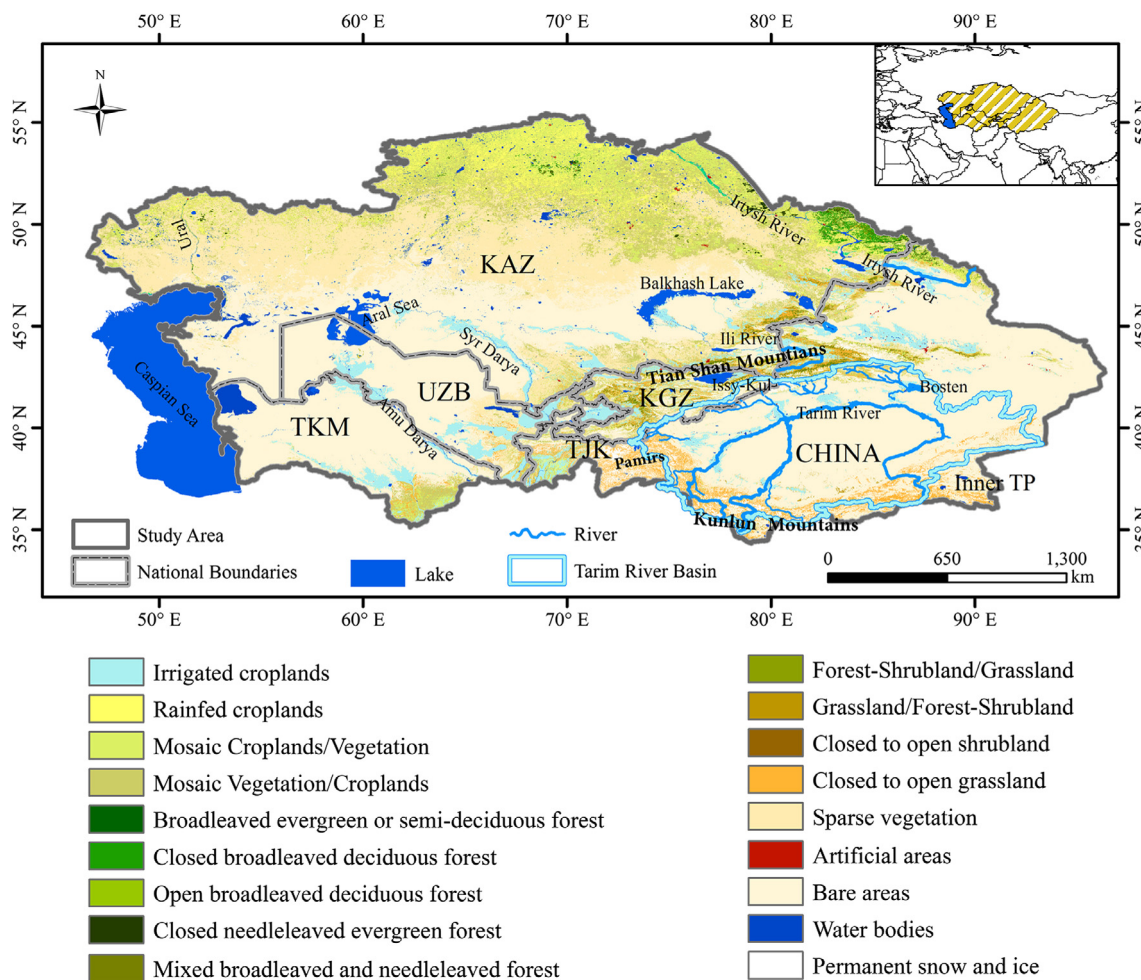


Fig. 1. Study area. This study area includes Kazakhstan (KAZ), Kyrgyzstan (KGZ), Tajikistan (TJK), Uzbekistan (UZB), Turkmenistan (TKM), and Xinjiang province in China. The vector data sources were supported by National Science & Technology Infrastructure of China, Data Sharing Infrastructure of Earth System Science (<http://www.geodata.cn>). The land cover dataset from 2009 was supported by the USGS Land Cover Institute (http://due.esrin.esa.int/page_globcover.php).

(Level-2 products) from January 2003 to December 2013, for a total of 124 months. Dating was missing for eight months (June 2003, January and June 2011, May and October 2012, and March, August, and September 2013).

2.2.2. GLDAS data

In this study, data for soil moisture content, evapotranspiration and snow water equivalent come from the Global Land Data Assimilation Systems (GLDAS) Noah land surface model (<http://disc.sci.gsfc.nasa.gov/services/grads-gds/gldas>). As with GRACE, the GLDAS dataset is set at a spatial resolution of 1 by 1 degrees. The 2-meter soil depth contains four soil layers (Rodell et al., 2004), so the four soil layers were calculated as the total soil moisture content.

2.2.3. Climate data

The monthly precipitation and temperature data are obtained from the high resolution gridded dataset supported by the Climatic Research Unit (CRU TS v.3.22), University of East Anglia (available at <http://www.cru.uea.ac.uk/cru/data/hrg/>). The CRU dataset covers all land areas (except Antarctica) from 1901 to 2013 (at a spa-

tial resolution of 0.5 by 0.5 degrees) and is based on monthly observational data from land meteorological stations across the world. Overall, it is generally in good agreement with other datasets such as GPCC (Harris et al., 2014).

2.3. Methods

2.3.1. Terrestrial water storage calculations

The monthly GRACE gravity spherical harmonics coefficients (Stokes' coefficients) in this study were provided by CSR. Wahr et al. (1998) pointed out that, according to the GRACE satellite data on the gravity spherical harmonic coefficients at monthly time-scales, land water storage is able to recover. The Earth's oblateness values (C20) coefficients were replaced in the GRACE data because the C20 values have larger uncertainty (Chen et al., 2005; Cheng and Tapley, 2000, 2004). The decorrelation algorithm supported by Swenson and Wahr (2006) is then used to remove the longitudinal stripe error effects. Finally, the Gaussian averaging filter with a smoothing radius of 300 km is applied to calculate the TWS, i.e., the equivalent water height, based on the gravity spherical harmonic coefficients (Swenson and Wahr, 2006). Therefore, the

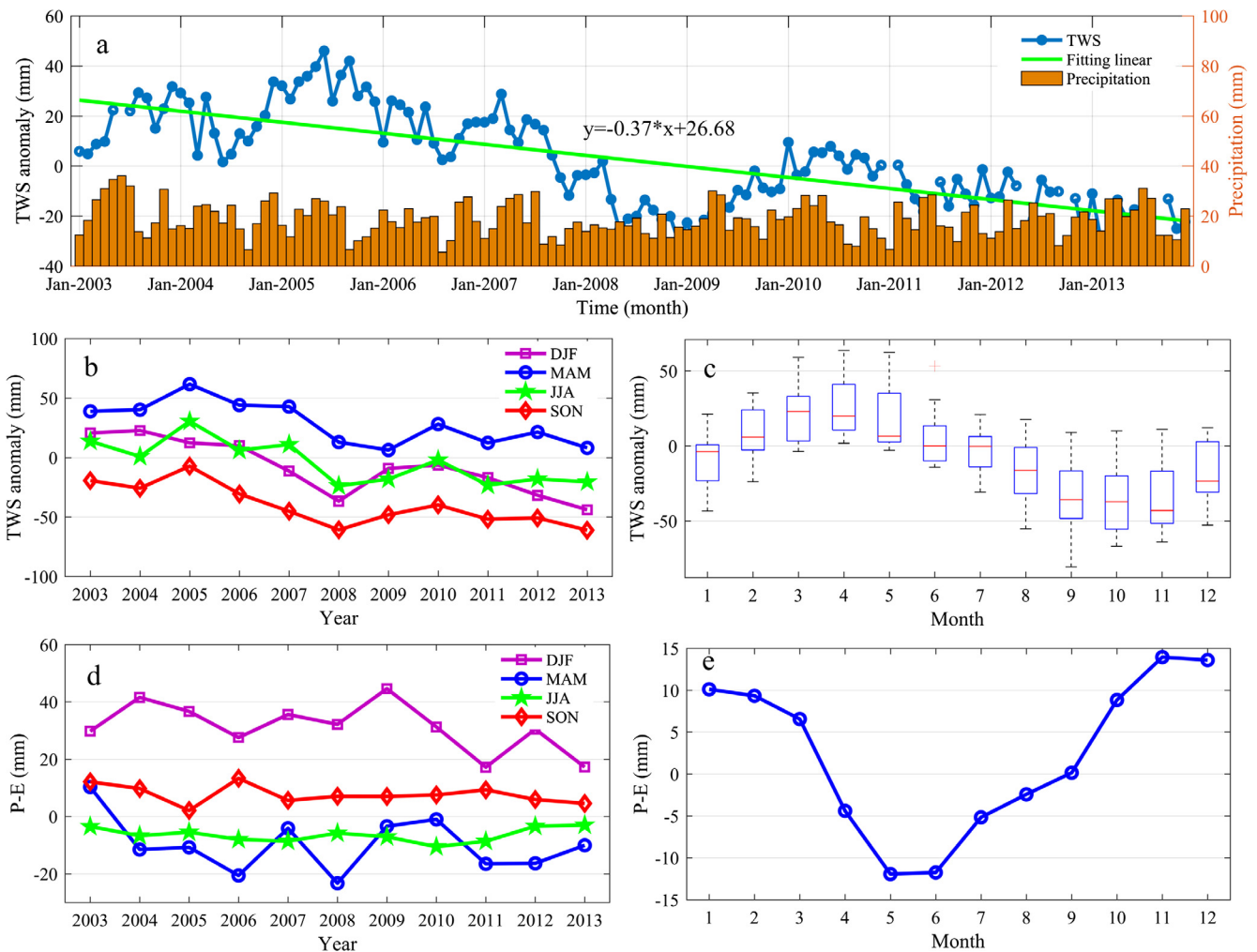


Fig. 2. Temporal variability of terrestrial water storage in Central Asia: (a) is terrestrial water storage variations in Central Asia estimated by GRACE data from January 2003 to December 2013; the blue curve is terrestrial water storage estimated by GRACE; the inter-annual and seasonal means of GRACE TWS have been removed before fitting linear; (b) shows seasonal TWS variations from 2003 to 2013, DJF (from December to February), MAM (from March to May), JJA (from June to August), and SON (from September to November); (c) shows year-to-year changes in monthly TWS, the thick horizontal lines represent the month's median TWS, the boxes show the inner-quartile range, the whiskers show the full range of the data, the red plus sign shows the extreme values; (d) shows the seasonal P-E (precipitation minus evapotranspiration) variations from 2003 to 2013, and (e) is year-to-year changes in monthly P-E. (For interpretation of the references to color in this figure legend, the reader is referred to the web version of this article.)

TWS is actually the equivalent water height calculated based on gravity spherical harmonic coefficients by the following equation (Wahr et al., 1998):

$$\Delta\varphi(\theta, \phi) = a\rho_{ave}/3 \sum_{n=0}^{\infty} \sum_{m=0}^n (2n+1)/(1+k_n) (\Delta C_{nm} \cos(m\phi) + \Delta S_{nm} \sin(m\phi)) P_{nm}(\sin(\theta)) \quad (1)$$

where φ is equivalent water height, θ is the latitude, ϕ is the longitude, a is the equatorial radius, ρ_{ave} is the mean density of Earth, k_n is the love number, C_{nm} and S_{nm} are the coefficients of the spherical harmonics (Stokes' coefficients), and $P_{nm}(\sin(\theta))$ is the n th degree and m th order fully-normalized Legendre function, with maximum degree n and order m , expanded to 60.

Scaling factors of each grid cell were calculated by the following equation (Landerer and Swenson, 2012):

$$M = \sum_i^t (\Delta S_{T,i} - k\Delta S_{F,i})^2 \quad (2)$$

where t is the total months used in this study, $\Delta S_{T,i}$ is the i months unfiltered CLM4.0 TWS anomalies, $\Delta S_{F,i}$ is the i months filtered CLM4.0 TWS anomalies processed in the same way as the filtered GRACE data, k is scaling factors derived from least square regression, and M is objective function. The scaling factors are provided by the JPL website (ftp://podaac-ftp.jpl.nasa.gov/allData/telus/L3/land_mass/RL05/netcdf/).

Errors in estimated TWS variations mainly include measurement errors in the monthly GRACE gravity field solutions (Wahr et al., 2006) and leakage errors (Long et al., 2015). In this study, areas such as the Caspian Sea region and transition regions between mountains and plains should be considered to reduce leakage error effects. The leakage errors of each grid cell were calculated by the following equation (Landerer and Swenson, 2012):

$$E_g^l = RMS(\Delta S_T - k\Delta S_F) \frac{RMS_{GRACE}}{RMS_{model}} \quad (3)$$

where ΔS_T and ΔS_F are defined in Eq. (2) and k is the scaling factor calculated in Eq. (2).

Next, the total errors of each grid were estimated by leakage and measurement errors, summed in the quadrature (Landerer and Swenson, 2012) in Eq. (4).

$$e_{total} = \sqrt{L_e^2 + M_e^2} \quad (4)$$

where e_{total} is the present total errors of each grid cell, and L_e and M_e are the current leakage errors and measurement errors of each grid cell, respectively. The measurement errors and leakage errors are provided at the JPL website (<http://grace.jpl.nasa.gov/data/get-data/monthly-mass-grids-land/>).

2.3.2. Mann-Kendal trend test

The Mann-Kendall nonparametric trend test is commonly used to assess the significance of trends in meteorological and hydro-

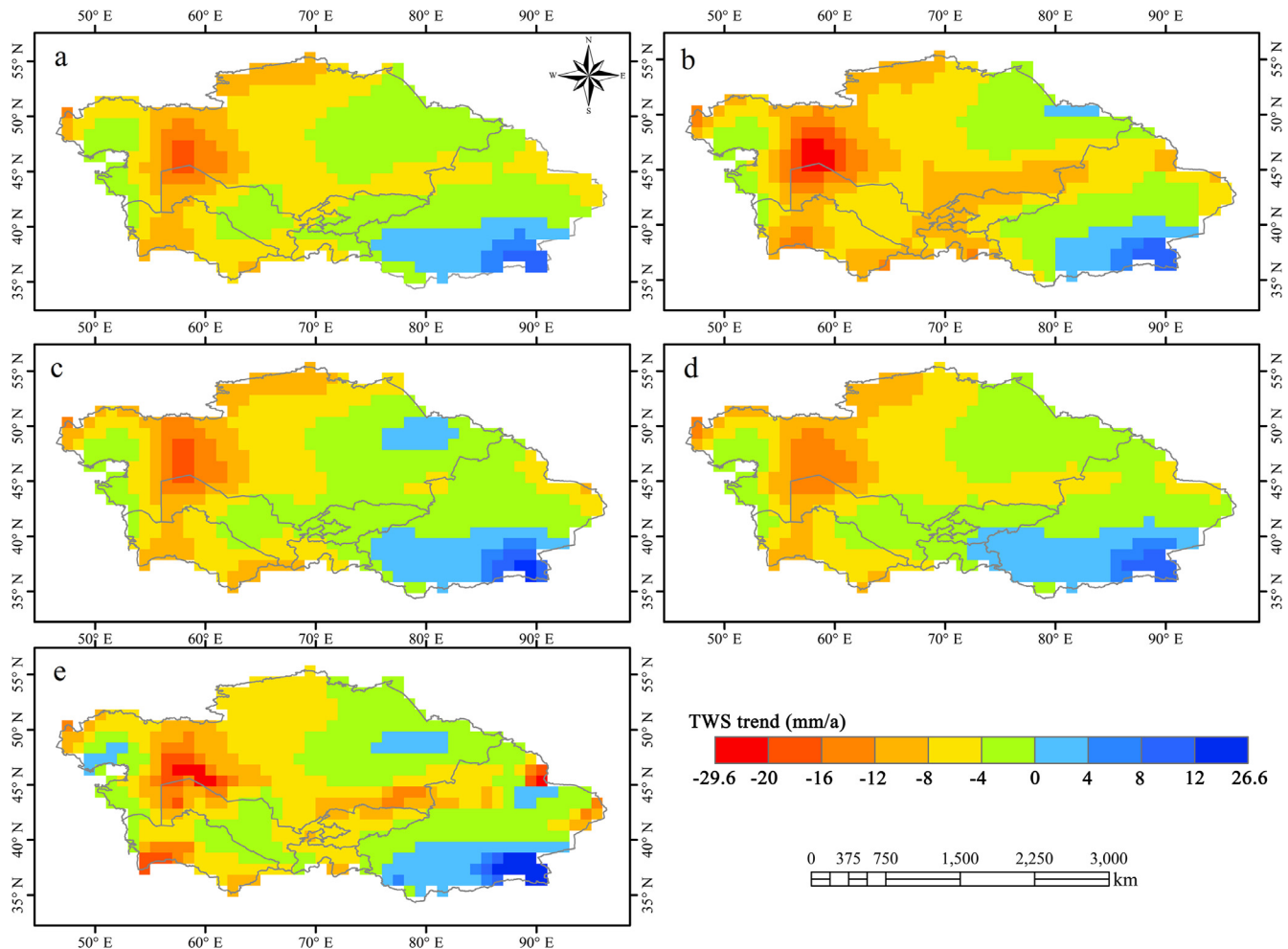


Fig. 3. Spatial variability of terrestrial water storage in Central Asia: (a) is annual spatial variations of total water storage in Central Asia from 2003 to 2013; (b–e) show seasonal spatial variations in terrestrial water storage in DJF, MAM, JJA, and SON, respectively.

logic time series data (e.g., Hirsch and Slack, 1984; Hamed and Ramachandra Rao, 1998; Hamed, 2008). Here, we used the M-K trend method to detect TWS, temperature, and precipitation trends in Central Asia.

3. Results

3.1. TWS variations

TWS anomalies in the GRACE dataset (Fig. 2a) show a decreasing trend from January 2003 to December 2013 ($y = -0.37x + 26.68$), with a decline of -4.44 ± 2.2 mm/a. The maximum positive anomaly of TWS is larger than 40 mm and occurred in July 2005, while the minimum negative anomaly of about -20 mm occurred in March 2008–August 2009.

The seasonal analysis results indicate that there were seasonal differences in TWS variations in Central Asia over the past decade. Fig. 2b shows that TWS had a positive anomaly in MAM (30.3 mm) and a negative anomaly in SON (-48.7 mm), while TWS in DJF and JJA was stable compared to MAM and SON (Fig. 2b). Fig. 2b also shows that TWS in Central Asia presented a decreasing trend across all seasons from 2003 to 2013.

Fig. 2c shows year-to-year variability in monthly TWS anomalies in Central Asia from 2003 to 2013. The results show that variability in monthly TWS anomalies was larger during the spring months (March–May) than the autumn months (September–November). Precipitation and evapotranspiration have obvious seasonal differences. Water storage in general is equal to precipitation minus evapotranspiration (hereafter referred to as P–E) in Central Asia, mainly because this region comprises interior drainage basins. Fig. 2d shows positive differences for P–E in DJF and SON,

and negative differences in MAM and JJA. The differences in monthly P–E were negative for the summer half of the year (from mid-March to the end of August), but positive in the winter half (Fig. 2e).

Spatial variations in TWS indicate that there were significant spatial differences for the sub-region of Central Asia (Fig. 3a). Fig. 3a shows that TWS experienced a decreasing trend across Central Asia, while the southeastern regions (i.e., the southern Tarim River Basin and Inner Tibetan Plateau) had an increasing rate of 0 – 12 mm/a. In addition, these results show that most of the regions have a declining rate (0 to -8 mm/a), with western Central Asia (i.e., the Aral Sea region) showing the largest declining rate (-16 to -20 mm/a). The overall negative trend in water storage in this area is closely related to the shrinking of the Aral Sea (Singh et al., 2012).

Seasonal spatial analysis results illustrates that TWS variations in western Central Asia experienced a largest decreasing trend throughout all the seasons: DJF (Fig. 3b), MAM (Fig. 3c), JJA (Fig. 3d) and SON (Fig. 3e), with a declining rate of -16 to -29.6 mm/a. The Tian Shan Mountains region also showed a decreasing trend (0 to -12 mm/a) across all seasons (Fig. 3b–e). The decreasing trend for DJF and SON was larger than in MAM and JJA. However, seasonal variations in TWS south of the Tarim River Basin showed a significant increasing trend across all seasons (Fig. 3b–e) at a rate of 0 – 26.6 mm/a, with some regions in the Irtysh River Basin showing an increasing trend in DJF (Fig. 3b), MAM (Fig. 3c), and SON (Fig. 3e).

In addition, Fig. 2a indicates that time-series variations in TWS were related to factors such as precipitation. As defined in the water balance equation, precipitation (both solid and liquid) is an input variable to water systems (Davie, 2008). Temperature also affects TWS variations.

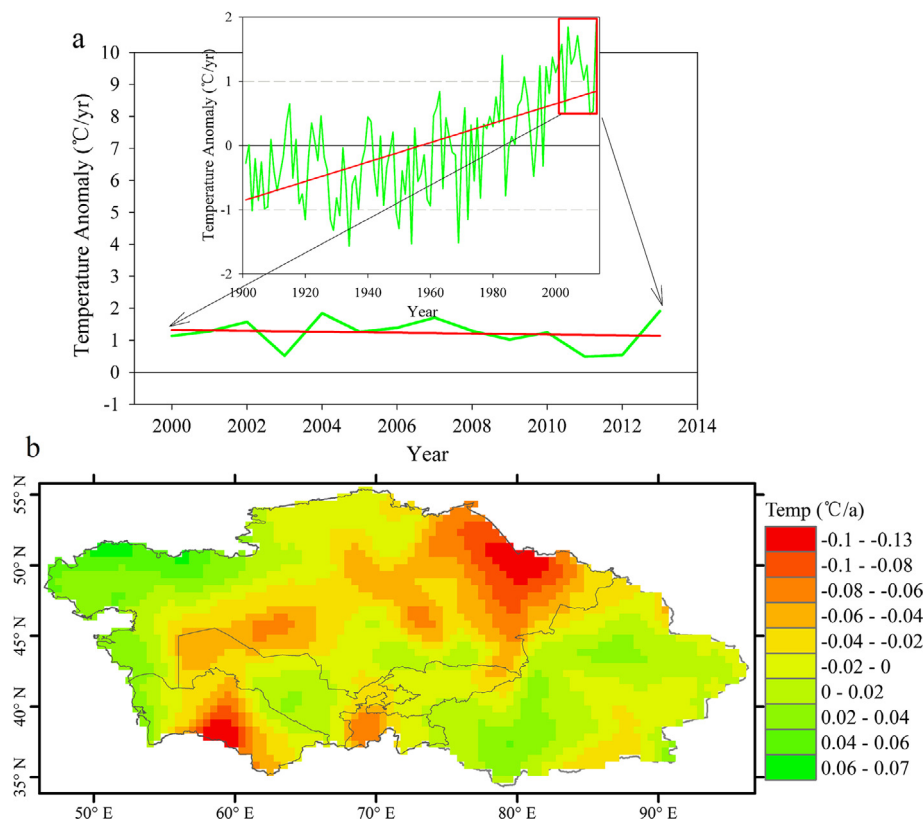


Fig. 4. Spatio-temporal variability of annual temperature in Central Asia. (a) Annual temperature trends in Central Asia during 1901–2013, based on CRU datasets. The green line is the time-series and the red line indicates annual temperature trends. The red box shows the annual temperature time-series from 2000 to 2013. (b) Spatial variations in annual temperature during 2000–2013, based on CRU datasets. (For interpretation of the references to color in this figure legend, the reader is referred to the web version of this article.)

3.2. Air temperature and precipitation changes

3.2.1. Air temperature

According to CRU data for Central Asia, anomalies in annual mean air temperature reveal an obvious change around 1960, from a negative phase to a positive one (Fig. 4a). The results indicate that while annual temperature experienced an increasing trend from 1901 to 2013, the trend was especially notable from 1960 to 2013. Over the past century, the average annual temperature increase in Central Asia measured 0.15 °C/decade, while the increase from 1960 to 2013 was 0.31 °C/decade (Fig. 4a). However, from 2000 to 2013, the increasing trend in annual temperature (Fig. 4a) was less pronounced than in previous years. The results show that the regions experiencing annual temperature increases were mainly located in the Ural River Basin and Xinjiang province of China and did not pass the 0.05 significance level (Fig. 4b). Moreover, annual temperatures in the Irtysh River Basin and northern Kazakhstan actually decreased from 2000 to 2013 and also did not pass the 0.05 significance level, except for the midstream and upstream areas of the Amu Darya River Basin (Fig. 4b).

3.2.2. Precipitation

Changes in precipitation were investigated based on CRU datasets for Central Asia from 1901 to 2013. Annual precipitation was below 300 mm, while in areas of weak precipitation (e.g., the Taklimakan Desert), annual precipitation was below 150 mm. Meanwhile, in the upwind slope of the mountains, annual precipitation exceeded 400 mm, ranging from 400 mm to

900 mm. The overall results reveal that annual precipitation slightly increased 1.5 mm/decade (Fig. 5a). Anomalies in annual precipitation ranged from –60 mm to 40 mm during 1901–1955, whereas during 1956–2013, anomalies ranged from –58 mm to 70 mm (Fig. 5a), with an increasing rate of 2.3 mm/decade. The increasing trend of annual precipitation was discontinued between 2000 and 2013 (Fig. 5a).

Additionally, we analyzed spatial variations in annual precipitation in Central Asia from 2000 to 2013 (Fig. 5b). Results show that an increasing trend occurred in the Tarim Basin (0–3 mm/a), the Junggar Basin (3–6 mm/a), and the midstream area of the Amu Darya River Basin (0–3 mm/a). However, annual precipitation decreased in the upstream portion of the Amu Darya River Basin (–6 to –9 mm/a) as well as in northwestern Kazakhstan (–3 to –6 mm/a) and eastern Central Asia (–9 to –12 mm/a).

3.3. Effects of climate change on TWS

Climate change is an important factor affecting TWS variations. The correlation coefficients between TWS anomalies and precipitation and temperature were calculated using monthly data. Fig. 6a shows that there was a significant negative correlation between TWS and temperature in northern Kazakhstan, with a correlation coefficient of –0.2 to –0.38, and $p < 0.05$, whereas in the southwestern (Turkmenistan and Uzbekistan) and southeastern regions (the Tarim River Basin), there were positive correlations, with a correlation coefficient of 0.3 to 0.48 and $p < 0.05$ (Fig. 6a). Fig. 6b shows that TWS had significant positive correlations with precipi-

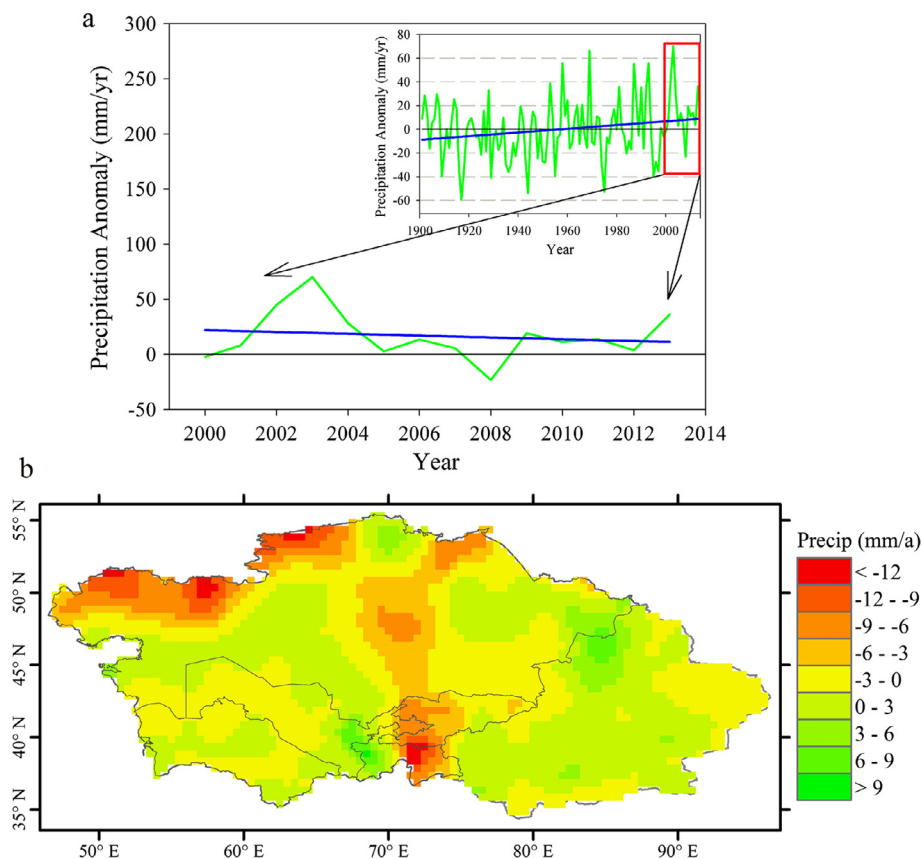


Fig. 5. Spatio-temporal variations in annual precipitation in Central Asia during 1901–2013, according to CRU datasets. The green line is the time-series and the blue line indicates annual precipitation trends. The red box shows the annual precipitation time-series from 2000 to 2013. (b) Spatial variations in annual precipitation during 2000–2013 by CRU datasets. (For interpretation of the references to color in this figure legend, the reader is referred to the web version of this article.)

tation in southeastern Kazakhstan (0.3–0.48, $p < 0.05$), Kyrgyzstan (0.2–0.3, $p < 0.05$), Tajikistan (0.3–0.4, $p < 0.05$), and the Tarim River Basin (0.3–0.4, $p < 0.05$). In the region’s northern parts, however, there were negative correlations, although none achieves a $p < 0.05$ significance level.

In the northern regions, there were negative correlations (–0.3 to –0.38) between TWS and T variations (Fig. 6a). Results in Fig. 7a reveal a decreasing trend in TWS anomalies in northern Central Asia (about –3.86 mm/a). Fig. 7b shows a trend towards decreasing precipitation and increasing evapotranspiration as well as a temperature decrease in the region (Fig. 7b). The increase in evapotranspiration was probably caused by increasing wind speeds (Fig. A.1). At the same time, changes in snow water equivalent (SWE) anomalies were relatively stable (Fig. 7c), and thus the decrease in precipitation and increase in evapotranspiration probably led to a change in soil moisture of about –4.95 mm/a (Fig. 7c). In northern Central Asia, changes in TWS anomalies are highly related to changes in soil moisture (Fig. 7d), with a correlation coefficient of 0.91. Therefore, the negative anomalies of TWS in this area were probably attributed to soil moisture storage loss.

In the Tian Shan Mountains region, the TWS anomalies declined by –3.6 mm/a from 2003 to 2013 (Fig. 3). This indicates an average water loss rate of -1.1 ± 0.64 Gt/a from 2003 to 2013, which is consistent with previous studies (Jacob et al., 2012). The total glacier area in the Tian Shans is 1.36×10^4 km² (RGI 5.0, Arendt et al., 2015). Farinotti et al.’s (2015) results point to a negative glacier

mass balance in the region from 2003 to 2009, with a retreat rate of -6.6 ± 4 Gt/a. Glacial mass loss in the Tian Shan Mountains was driven by climatic warming over the past few decades.

3.4. Effects of human activities on TWS

There were notable spatial differences in the TWS variations in the Tarim River Basin: the TWS increased in the southern areas and decreased in the northern areas (Fig. 3a–e). Furthermore, the results indicate that there is a positive correlation (0.3–0.4) between precipitation and TWS anomalies (Fig. 6b). However, the annual precipitation is less than 100 mm, which is less than is required to compensate for annual evapotranspiration (McVicar et al., 2012). In addition, there are large irrigation areas in the Tarim River Basin (Fig. 1); irrigation has expanded there over the past decades, with agricultural water consumption increasing by nearly 30% (Xu et al., 2013). Based on in-situ groundwater table measurements from 2004 to 2010, groundwater levels have undergone a rapid decline north of the Tarim River Basin (–1.5 m/a, Fig. 8a) and a slow decline west of the Basin (–0.3 m/a, Fig. 8b).

Table 2 shows that groundwater withdrawal increased in the northern Tarim River Basin and decreased in the south. Groundwater withdrawal in the Kaidu-Kongqa River basin in 2013 was 3.3 times that of 2007, in the Aksu River basin it was 2.2 times that of 2007, and withdrawal in the Yarkant River basin increased by 77% from the 2007 rate. However, groundwater withdrawal in the Hotan

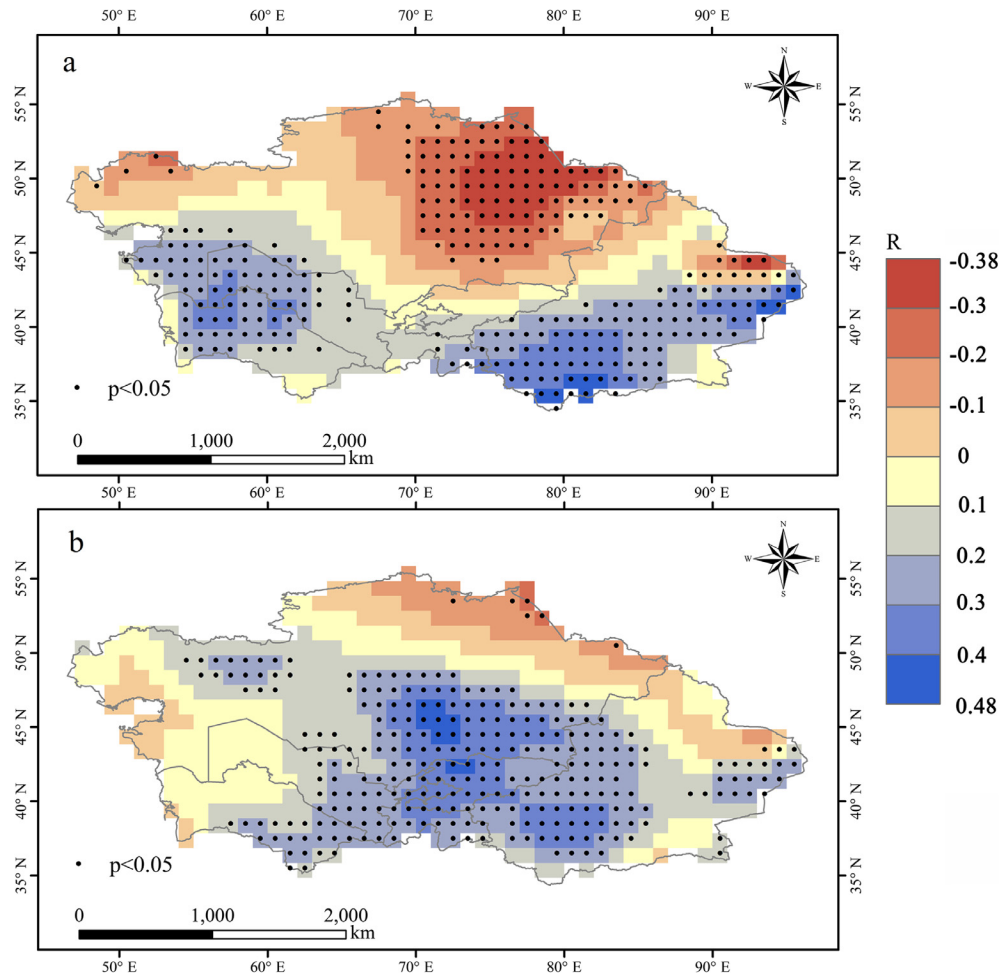


Fig. 6. Analysis of relationship between TWS and temperature and precipitation in Central Asia: (a) shows the Spearman correlations between TWS and temperature in Central Asia, while (b) shows the Spearman correlations between TWS and precipitation. The black dot signs represent significant correlations at levels of $p < 0.05$ from 2000 to 2013.

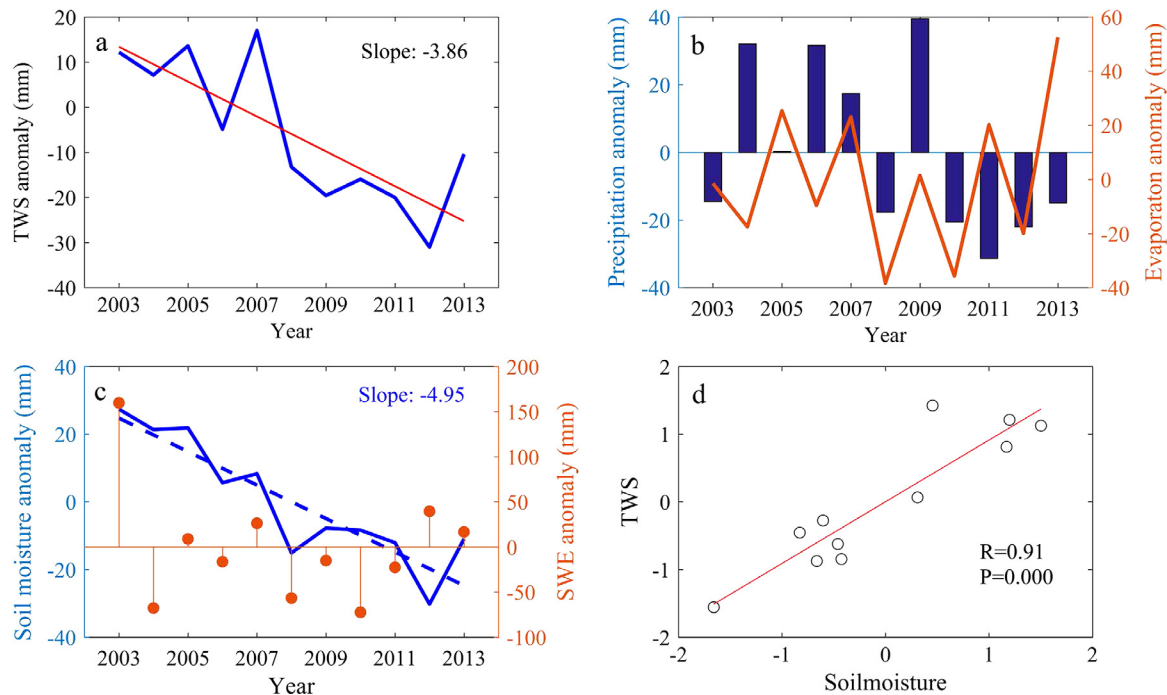


Fig. 7. Analysis of TWS variations in northern Central Asia from 2003 to 2013: (a) is annual TWS variations; (b) is anomalies of precipitation and evapotranspiration; (c) is anomalies of annual soil moisture and snow water equivalent (SWE); and (d) is correlation of TWS and soil moisture. The precipitation data was from CRU (<http://www.cru.uea.ac.uk/cru/data/hrg/>), while the evapotranspiration, soil moisture and SWE data were provided by GLDAS (<http://disc.sci.gsfc.nasa.gov/services/grads-gds/gldas>).

River basin decreased by 37% in 2013 compared to 2007. Therefore the excessive withdrawal of groundwater directly caused the decrease in groundwater storage in the northern Tarim River Basin.

4. Discussion

4.1. Spatial-temporal changes in TWS

Over the past 10 years, TWS in Central Asia has declined at a rate of -4.44 ± 2.2 mm/a. There are obvious differences between TWS (Fig. 2c) and P-E (Fig. 2e) on an inter-annual scale. These are attributable to the accumulation of negative differences in P-E from March to August, which then lead to a maximum negative anomaly for TWS occurring in September. Likewise, the accumulation of positive differences in P-E from September to March (in the subsequent year) then led a maximum positive anomaly of TWS in April. Table 3 shows a comprehensive evaluation of annual TWS variations for the Central Asian sub-regions. TWS decreased in northern Central Asia (-3.86 ± 0.63 mm/a) and the Tian Shan Mountains (-3.6 ± 0.32 mm/a), and both of these decreases were driven by climate change. However, decreases in TWS in the Aral Sea region (-10.68 ± 41.47 mm/a) and the northern Tarim River Basin (-0.82 ± 0.09 mm/a) were driven by human activities. It is worth noting that while there is larger uncertainty in TWS (about 41.5 mm/a) in the Aral Sea, this is probably caused by significant measurement errors in the region.

Mid-latitude regions are topographically complex, so changes in TWS in these areas are the result of several interacting factors. In low latitude regions, variations in TWS are mainly attributed to precipitation (Syed et al., 2008), whereas in high latitude regions, snow cover is the main factor (Ramillien et al., 2005). Yang et al. (2015) pointed out that increasing subsurface water (6.9 ± 2.2 mm/a) led to increases in TWS in the Tarim River Basin from 2005 to 2011. However, this is inconsistent with the in-situ measured groundwater table measurements (Fig. 8a and b). Our

results show that groundwater levels decreased in the northern and western Tarim River Basin, but increased in the south.

4.2. Effects of human activities

The shrinking of lakes also contributed to negative TWS anomalies in western Central Asia. The Aral Sea shrank from 5.93×10^4 km² in 1975 to 1.44×10^4 km² in 2007, a decrease of 75.7% (Bai et al., 2011). By the mid-1980s, water loss in the Aral Sea due to agricultural diversion resulted in the lake dividing into two smaller lakes: The South Aral Sea and the North Aral Sea (Singh et al., 2012; Shi et al., 2014). From 1993 to 2013, the total water storage loss in the South Aral Sea was approximately 200 km³, but the North Aral Sea has remained relatively stable during the same time period (Shi et al., 2014).

Lake area shrinkage in Central Asia is caused primarily by climate change and human activities. However, since the mid-1980s, anthropogenic influence has been the dominant factor (Micklin, 2010). The irrigated areas are mainly distributed in the Amu Darya Basin and the Syr Darya Basin (Fig. 1). Variations in TWS anomalies in the Aral Sea are in good agreement with runoff changes in the Syr Darya (Singh et al., 2012). Irrigation increased by 60% in Central Asia from 1962 to 2002 (FAO, 2004; Oberhansli et al., 2007), causing a reduction in the inflow water in the Aral Sea and an increase in groundwater withdrawals (Shibuo et al., 2006).

4.3. Effects of glacier retreat

Glaciers and snow cover are the main forms of TWS in mountainous regions, but global climate change has resulted in the shrinking of glaciers in the Tian Shan Mountains (Farinotti et al., 2015; Sorg et al., 2012). During the last decade, glacier mass balance retreat was measured at about 5 ± 6 billion cubic meters (Jacob et al., 2012). At the same time, the snow/precipitation ratio

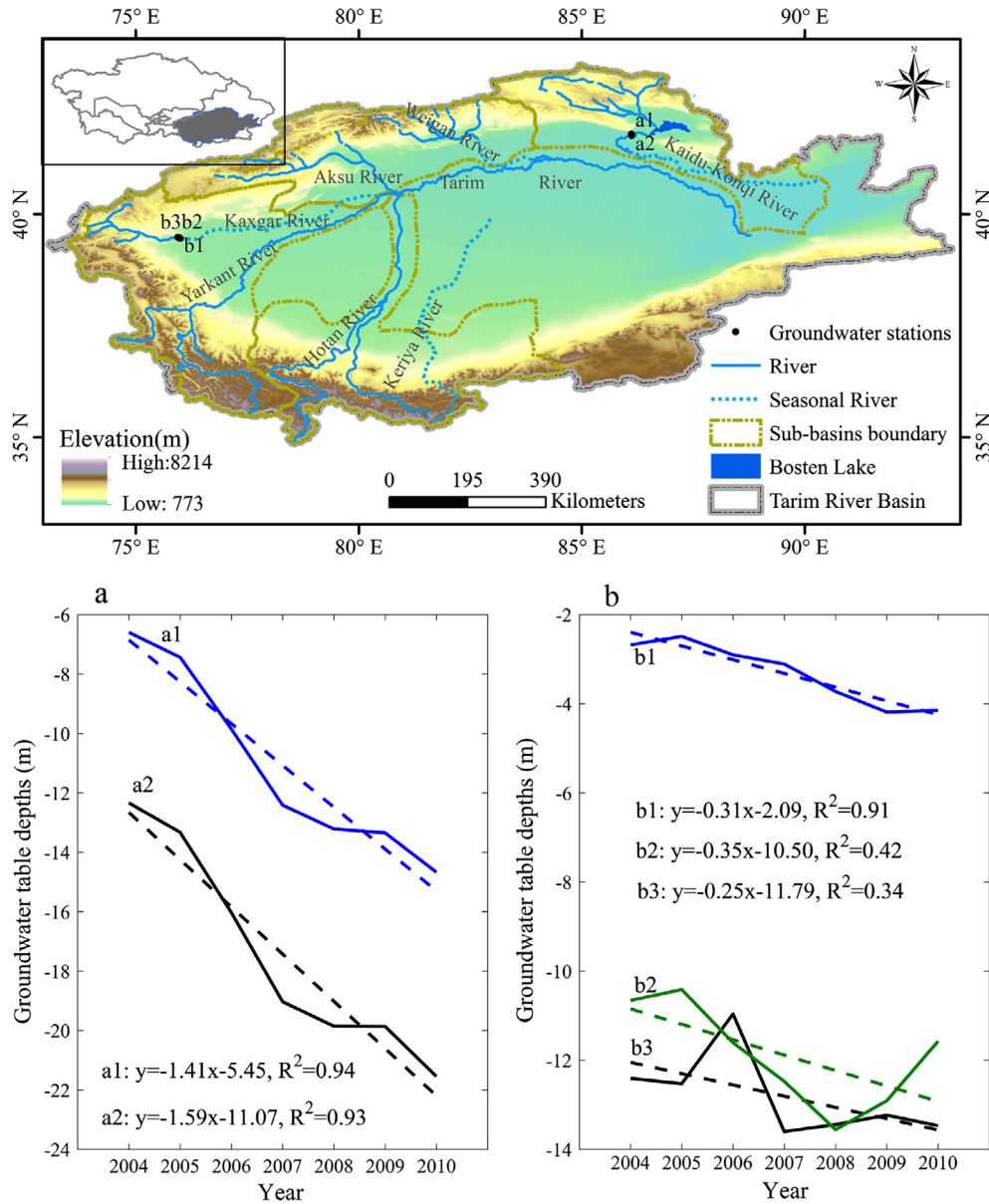


Fig. 8. Changes in the groundwater table based on in situ station data in the Tarim River Basin from 2004 to 2010. The groundwater table data is provided by the China Geological Environment Information, China Institute of Geo-Environment Monitoring (CIGEM) (<http://yj.cigem.gov.cn/dxs/Xinjiang.htm>).

Table 2
Groundwater withdrawal in the Tarim River Basin during 2007–2013 (unit: 10^8 m^3).

Basins	2007	2008	2009	2010	2011	2012	2013
Kaidu-Konqi River	4.26	6.61	8.29	9.01	9.01	13.79	13.99
Aksu River	4.31	4.58	6.42	7.05	6.85	8.62	9.33
Yarkant River	10.82	15.19	20.70	20.95	20.05	18.84	19.19
Hotan River	3.31	2.85	3.40	3.74	2.630	2.36	2.09

Groundwater withdrawal data are from the water resources bulletin of Xinjiang province in 2007, 2008, 2009, 2010, 2011, 2012, and 2013 (<http://www.xjslt.gov.cn/szygb/index.htm>). The Kaidu-Konqi River, Aksu River, Yarkant River, and Hotan River are illustrated in Fig. 8.

Table 3
Trend analysis and influence factors of annual TWS variations in sub-regions of Central Asia during 2003–2013. Here, the uncertainty includes measurement error, and seasonal and inter-annual variability (Wahr et al., 2006).

Regional	Trend (mm/a)	Dominate factors	Manifestations
North of CA	-3.86 ± 0.63	Climate change	Soil moisture loss
Tian Shan Mountains	-3.6 ± 0.32	Climate change	Glaciers retreat
Aral Sea region	-10.68 ± 41.47	Human activities	Lake shrunk and GW overexploitation
North of TRB	-0.82 ± 0.09	Human activities	GW overexploitation

CA and TRB are abbreviations for Central Asia and Tarim River Basin, respectively; GW overexploitation represents groundwater overexploitation.

for total precipitation exhibited a downward trend (Guo and Li, 2015), as did snow meltwater. The data indicate that the glacier retreat in the Tian Shan Mountains along with the decreasing snow/precipitation ratio caused a downward trend in TWS. The most important signal is the increasing trend presented by glaciers in the western Kunlun Mountains. During 2002–2010, there was a positive mass balance increase in the Muztag Ata glacier (38°14' N, 75°03' E) in the western Kunlun Mountains at an average of +250 mm yr⁻¹ (Yao et al., 2012), which consequently contributed to an increase in TWS in the southern Tarim River Basin (Fig. 3). From these data, we can conclude that climate change affected TWS by influencing changes in mountain glaciers and snow cover.

5. Conclusions

In this study, the influence of recent climate change and human activities on TWS variations from 2003 to 2013 was analyzed for Central Asia. The main results are as follows:

1. Over the past decade, TWS variations presented a decreasing trend at a rate of -4.44 ± 2.2 mm/a;
2. The seasonal analysis results indicated that there were seasonal differences in variations in TWS over the past decade. Specifically, TWS showed a positive anomaly in MAM (30.3 mm) and a negative one in SON (−48.7 mm);
3. The declining rates of TWS in western and northern Central Asia, the Tian Shan Mountains, and the northern Tarim River Basin are -10.68 mm/a, -3.86 mm/a, -3.6 mm/a, and 0.82 mm/a, respectively;
4. In the Tian Shan Mountains, there was an average water loss rate of -1.1 ± 0.64 Gt/a during 2003–2013;
5. TWS increased in the southern Tarim River Basin, which was mainly caused by the increase in groundwater and positive mass balance of glaciers;
6. Decreases in TWS in northern Central Asia and the Tian Shan Mountains were driven by climate factors, while decreases in western Central Asia and the northern Tarim River Basin were driven by human activities.

Acknowledgements

This research is supported by the National Natural Science Foundation of China (No. 41630859, and No. 41471030), and the Foundation of the CAS “Light of West China” Program (2015-XBQN-B-17). The GRACE land data are available at <http://grace.jpl.nasa.gov>, supported by the NASA MEASURES Program. The groundwater table data are provided by the China Geological Environment Information, China Institute of Geo-Environment Monitoring (CIGEM) (<http://yj.cigem.gov.cn/dxs/Xinjiang.htm>). The authors appreciate the comments and encouragement given by the reviewers, editor, and associate editor.

Appendix A. Supplementary material

Supplementary data associated with this article can be found, in the online version, at <http://dx.doi.org/10.1016/j.jhydrol.2016.11.006>.

References

Aizen, V.B., Aizen, E.M., Melack, J.M., Dozier, J., 1997. Climatic and hydrologic changes in the Tien Shan, Central Asia. *J. Clim.* 10 (6), 1393–1404. [http://dx.doi.org/10.1175/1520-0442\(1997\)010<1393:CAHCIT>2.0.CO;2](http://dx.doi.org/10.1175/1520-0442(1997)010<1393:CAHCIT>2.0.CO;2).

Arendt, A., Bliss, A., Bolch, T., Cogley, J.G., Gardner, A.S., O'Hagen, J., Ellipsis Zhelytshina, N., 2015. Randolph Glacier Inventory – A Dataset of Global Glacier

Outlines: Version 5.0. Global Land Ice Measurements from Space, Boulder Colorado, USA. Digital Media.

Bai, J., Chen, X., Li, J., Yang, L., Fang, H., 2011. Changes in the area of inland lakes in arid regions of central Asia during the past 30 years. *Environ. Monit. Assess* 178 (1), 247–256. <http://dx.doi.org/10.1007/s10661-010-1686-y>.

Bernauer, T., Siegfried, T., 2012. Climate change and international water conflict in Central Asia. *J. Peace Res.* 49 (1), 227–239. <http://dx.doi.org/10.1177/0022343311425843>.

Cao, Y., Nan, Z., Cheng, G., 2015. GRACE gravity satellite observations of terrestrial water storage changes for drought characterization in the arid land of Northwestern China. *Remote Sensing* 7 (1), 1021–1047. <http://dx.doi.org/10.3390/rs70101021>.

Chen, J.L., Rodell, M., Wilson, C.R., Famiglietti, J.S., 2005. Low degree spherical harmonic influences on Gravity Recovery and Climate Experiment (GRACE) water storage estimates. *Geophys. Res. Lett.* 32 (14). <http://dx.doi.org/10.1029/2005GL022964>.

Chen, Y., Li, Z., Fan, Y., Wang, H., Deng, H., 2015. Progress and prospects of climate change impacts on hydrology in the arid region of northwest China. *Environ. Res.* 139, 11–19. <http://dx.doi.org/10.1016/j.envres.2014.12.029>.

Chen, Y., Li, Z., Li, W., Deng, H., Shen, Y., 2016. Water and ecological security: dealing with hydroclimatic challenges at the heart of China's Silk Road. *Environ. Earth Sci.* <http://dx.doi.org/10.1007/s12665-016-5385-z>.

Cheng, M., Tapley, B., 2000. Temporal variations in J2 from analysis of SLR data. In: Proc. 12th International Workshop on Laser Ranging.

Cheng, M., Tapley, B.D., 2004. Variations in the Earth's oblateness during the past 28 years. *J. Geophys. Res.: Solid Earth* 109 (B9), B09402. <http://dx.doi.org/10.1029/2004JB003028>.

Crowley, J.W., Mitrovica, J.X., Bailey, R.C., Tamisiea, M.E., Davis, J.L., 2006. Land water storage within the Congo Basin inferred from GRACE satellite gravity data. *Geophys. Res. Lett.* 33 (19), L19402. <http://dx.doi.org/10.1029/2006GL027070>.

Davie, T., 2008. *Fundamentals of hydrology*. Taylor & Francis, p. 11.

FAO, 2004. The State of World Fisheries and Aquaculture (SOFIA) 2004. Food and Agriculture Organization, Rome, Italy <<http://www.fao.org/publications/en/>>.

Farinotti, D., Longuevergne, L., Moholdt, G., Duethmann, D., Molg, T., Bolch, T., Vorogushyn, S., Guntner, A., 2015. Substantial glacier mass loss in the Tien Shan over the past 50 years. *Nat. Geosci.* 8 (9), 716–722. <http://dx.doi.org/10.1038/ngeo2513>.

Feng, W., Zhong, M., Lemoine, J.M., Biancale, R., Hsu, H.T., Xia, J., 2013. Evaluation of groundwater depletion in North China using the Gravity Recovery and Climate Experiment (GRACE) data and ground-based measurements. *Water Resour. Res.* 49 (4), 2110–2118. <http://dx.doi.org/10.1002/wrcr.20192>.

Grippa, M., Kergoat, L., Frappart, F., Araud, Q., Boone, A., de Rosnay, P., Lemoine, J.M., Gascoin, S., Balsamo, G., Otlé, C., Decharme, B., Saux-Picart, S., Ramillien, G., 2011. Land water storage variability over West Africa estimated by Gravity Recovery and Climate Experiment (GRACE) and land surface models. *Water Resour. Res.* 47 (5), W05549. <http://dx.doi.org/10.1029/2009WR008856>.

Guo, L., Li, L., 2015. Variation of the proportion of precipitation occurring as snow in the Tian Shan Mountains, China. *Int. J. Climatol.* 35 (7), 1379–1393. <http://dx.doi.org/10.1002/joc.4063>.

Hamed, K.H., 2008. Trend detection in hydrologic data: the Mann-Kendall trend test under the scaling hypothesis. *J. Hydrol.* 349 (3–4), 350–363. <http://dx.doi.org/10.1016/j.jhydrol.2007.11.009>.

Hamed, K.H., Ramachandra Rao, A., 1998. A modified Mann-Kendall trend test for autocorrelated data. *J. Hydrol.* 204 (1–4), 182–196. [http://dx.doi.org/10.1016/S0022-1694\(97\)00125-X](http://dx.doi.org/10.1016/S0022-1694(97)00125-X).

Harris, I., Jones, P.D., Osborn, T.J., Lister, D.H., 2014. Updated high-resolution grids of monthly climatic observations – the CRU TS3.10 Dataset. *Int. J. Climatol.* 34 (3), 623–642. <http://dx.doi.org/10.1002/joc.3711>.

Hirschi, M., Seneviratne, S.I., Schär, C., 2006. Seasonal variations in terrestrial water storage for major midlatitude river basins. *J. Hydrometeorol.* 7 (1), 39–60. <http://dx.doi.org/10.1175/JHM480.1>.

Hirsch, R.M., Slack, J.R., 1984. A nonparametric trend test for seasonal data with serial dependence. *Water Resour. Res.* 20 (6), 727–732. <http://dx.doi.org/10.1029/WR020i006p00727>.

Houborg, R., Rodell, M., Li, B., Reichle, R., Zaitchik, B.F., 2012. Drought indicators based on model-assimilated Gravity Recovery and Climate Experiment (GRACE) terrestrial water storage observations. *Water Resour. Res.* 48 (7), W07525. <http://dx.doi.org/10.1029/2011WR011291>.

Immerzeel, W.W., van Beek, L.P.H., Bierkens, M.F.P., 2010. Climate change will affect the Asian Water Towers. *Science* 328 (5984), 1382–1385. <http://dx.doi.org/10.1126/science.1183188>.

Jacob, T., Wahr, J., Pfeffer, W.T., Swenson, S., 2012. Recent contributions of glaciers and ice caps to sea level rise. *Nature* 482 (7386), 514–518. <http://dx.doi.org/10.1038/nature10847>.

Landerer, F.W., Swenson, S.C., 2012. Accuracy of scaled GRACE terrestrial water storage estimates. *Water Resour. Res.* 48 (4). <http://dx.doi.org/10.1029/2011WR011453>.

Li, Z., Chen, Y., Li, W., Deng, H., Fang, G., 2015. Potential impacts of climate change on vegetation dynamics in Central Asia. *J. Geophys. Res.* 120, 12345–12356. DOI: 10.1002-2015JD023618.

Lioubimtseva, E., Cole, R., Adams, J.M., Kapustin, G., 2005. Impacts of climate and land-cover changes in arid lands of Central Asia. *J. Arid Environ.* 62 (2), 285–308. <http://dx.doi.org/10.1016/j.jaridenv.2004.11.005>.

- Lioubimtseva, E., Henebry, G.M., 2009. Climate and environmental change in arid Central Asia: impacts, vulnerability, and adaptations. *J. Arid Environ.* 73 (11), 963–977. <http://dx.doi.org/10.1016/j.jaridenv.2009.04.022>.
- Long, D., Longuevergne, L., Scanlon, B.R., 2015. Global analysis of approaches for deriving total water storage changes from GRACE satellites. *Water Resour. Res.* 51 (4), 2574–2594. <http://dx.doi.org/10.1002/2014WR016853>.
- Long, D., Scanlon, B.R., Longuevergne, L., Sun, A.Y., Fernando, D.N., Save, H., 2013. GRACE satellite monitoring of large depletion in water storage in response to the 2011 drought in Texas. *Geophys. Res. Lett.* 40 (13), 3395–3401. <http://dx.doi.org/10.1002/grl.50655>.
- Long, D., Shen, Y., Sun, A., Hong, Y., Longuevergne, L., Yang, Y., Li, B., Chen, L., 2014. Drought and flood monitoring for a large karst plateau in Southwest China using extended GRACE data. *Remote Sens. Environ.* 155, 145–160. <http://dx.doi.org/10.1016/j.rse.2014.08.006>.
- Mannig, B., Müller, M., Starke, E., Merckenschlager, C., Mao, W., Zhi, X., Podzun, R., Jacob, D., Paeth, H., 2013. Dynamical downscaling of climate change in Central Asia. *Global Planetary Change* 110 (Part A), 26–39. <http://dx.doi.org/10.1016/j.gloplacha.2013.05.008>.
- Matsuo, K., Heki, K., 2010. Time-variable ice loss in Asian high mountains from satellite gravimetry. *Earth Planet. Sci. Lett.* 290 (1–2), 30–36. <http://dx.doi.org/10.1016/j.epsl.2009.11.053>.
- McVicar, T.R., Körner, C., 2013. On the use of elevation, altitude, and height in the ecological and climatological literature. *Oecologia* 171 (2), 335–337. <http://dx.doi.org/10.1007/s00442-012-2416-7>.
- McVicar, T.R., Roderick, M.L., Donohue, R.J., Van Niel, T.G., 2012. Less bluster ahead? Overlooked ecohydrological implications of global trends of terrestrial near-surface wind speeds. *Ecohydrology* 5 (4), 381–388. <http://dx.doi.org/10.1002/eco.1298>.
- Micklin, P., 2010. The past, present, and future Aral Sea. *Lakes Reservoirs: Res. Manage.* 15 (3), 193–213. <http://dx.doi.org/10.1111/j.1440-1770.2010.00437.x>.
- Oberhänsli, H., Boroffka, N., Sorrel, P., Krivonogov, S., 2007. Climate variability during the past 2,000 years and past economic and irrigation activities in the Aral Sea basin. *Irrigation Drainage Syst.* 21 (3–4), 167–183. <http://dx.doi.org/10.1007/s10795-007-9031-5>.
- Qi, J., Kulmatov, R., 2008. An overview of environmental issues in Central Asia. In: Qi, J., Evered, K. (Eds.), *Environmental Problems of Central Asia and Their Economic, Social and Security Impacts*. NATO Science for Peace and Security Series C: Environmental Security. Springer, Netherlands, pp. 3–14. http://dx.doi.org/10.1007/978-1-4020-8960-2_1.
- Ramillien, G., Frappart, F., Cazenave, A., Güntner, A., 2005. Time variations of land water storage from an inversion of 2 years of GRACE geoids. *Earth Planet. Sci. Lett.* 235 (1–2), 283–301. <http://dx.doi.org/10.1016/j.epsl.2005.04.005>.
- Rodell, M., Famiglietti, J.S., Chen, J., Seneviratne, S.I., Viterbo, P., Holl, S., Wilson, C.R., 2004. Basin scale estimates of evapotranspiration using GRACE and other observations. *Geophys. Res. Lett.* 31 (20). <http://dx.doi.org/10.1029/2004GL020873>.
- Rodell, M., Velicogna, I., Famiglietti, J.S., 2009. Satellite-based estimates of groundwater depletion in India. *Nature* 460 (7258), 999–1002. <http://dx.doi.org/10.1038/nature08238>.
- Shibuo, Y., Jarsjö, J., Destouni, G., 2006. Bathymetry-topography effects on saltwater–fresh groundwater interactions around the shrinking Aral Sea. *Water Resour. Res.* 42 (11). <http://dx.doi.org/10.1029/2005WR004207>.
- Shi, W., Wang, M., Guo, W., 2014. Long-term hydrological changes of the Aral Sea observed by satellites. *J. Geophys. Res.: Oceans* 119 (6), 3313–3326. <http://dx.doi.org/10.1002/2014JC009988>.
- Siegfried, T., Bernauer, T., Guiennet, R., Sellars, S., Robertson, A.W., Mankin, J., Bauer-Gottwein, P., Yakovlev, A., 2012. Will climate change exacerbate water stress in Central Asia? *Climatic Change* 112 (3–4), 881–899. <http://dx.doi.org/10.1007/s10584-011-0253-z>.
- Singh, A., Seitz, F., Schwatke, C., 2012. Inter-annual water storage changes in the Aral Sea from multi-mission satellite altimetry, optical remote sensing, and GRACE satellite gravimetry. *Remote Sens. Environ.* 123, 187–195. <http://dx.doi.org/10.1016/j.rse.2012.01.001>.
- Sorg, A., Bolch, T., Stoffel, M., Solomina, O., Beniston, M., 2012. Climate change impacts on glaciers and runoff in Tien Shan (Central Asia). *Nat. Clim. Change* 2 (10), 725–731. <http://dx.doi.org/10.1038/NCLIMATE1592>.
- Strassberg, G., Scanlon, B.R., Rodell, M., 2014. Comparison of seasonal terrestrial water storage variations from GRACE with groundwater-level measurements from the high plains aquifer (USA). *Geophys. Res. Lett.* 34 (14). <http://dx.doi.org/10.1029/2007GL030139>.
- Swenson, S.C., Wahr, J., 2006. Post-processing removal of correlated errors in GRACE data. *Geophys. Res. Lett.* 33, L08402. <http://dx.doi.org/10.1029/2005GL025285>.
- Swenson, S.C., 2012. GRACE monthly land water mass grids NETCDF RELEASE 5.0. Ver. 5.0. PO.DAAC, CA, USA. <http://dx.doi.org/10.5067/TELND-NC005> (last access: April 2016).
- Syed, T.H., Famiglietti, J.S., Rodell, M., Chen, J., Wilson, C.R., 2008. Analysis of terrestrial water storage changes from GRACE and GLDAS. *Water Resour. Res.* 44 (2), W02433. <http://dx.doi.org/10.1029/2006WR005779>.
- Tangdamrongsub, N., Steele-Dunne, S.C., Gunter, B.C., Ditmar, P.G., Weerts, A.H., 2015. Data assimilation of GRACE terrestrial water storage estimates into a regional hydrological model of the Rhine River basin. *Hydrol. Earth Syst. Sci.* 19 (4), 2079–2100. <http://dx.doi.org/10.5194/hess-19-2079-2015>.
- Thomas, A.C., Reager, J.T., Famiglietti, J.S., Rodell, M., 2014. A GRACE-based water storage deficit approach for hydrological drought characterization. *Geophys. Res. Lett.* 41 (5), 1537–1545. <http://dx.doi.org/10.1002/2014GL059323>.
- Wahr, J., Molenaar, M., Bryan, F., 1998. Time variability of the Earth's gravity field: hydrological and oceanic effects and their possible detection using GRACE. *J. Geophys. Res.: Solid Earth* 103 (B12), 30205–30229. <http://dx.doi.org/10.1029/98JB02844>.
- Wahr, J., Swenson, S., Velicogna, I., 2006. Accuracy of GRACE mass estimates. *Geophys. Res. Lett.* 33 (6). <http://dx.doi.org/10.1029/2005GL025305>.
- Xavier, L., Becker, M., Cazenave, A., Longuevergne, L., Llovel, W., Rotunno Filho, O.C., 2010. Interannual variability in water storage over 2003–2008 in the Amazon Basin from GRACE space gravimetry, in situ river level and precipitation data. *Remote Sens. Environ.* 114 (8), 1629–1637. <http://dx.doi.org/10.1016/j.rse.2010.02.005>.
- Xu, C., Chen, Y., Chen, Y., Zhao, R., Ding, H., 2013. Responses of surface runoff to climate change and human activities in the arid region of Central Asia: a case study in the Tarim river basin, China. *Environ. Manage.* 51 (4), 926–938. <http://dx.doi.org/10.1007/s00267-013-0018-8>.
- Yang, P., Chen, Y.N., 2015. An analysis of terrestrial water storage variations from GRACE and GLDAS: the Tianshan Mountains and its adjacent areas, central Asia. *Quaternary Int.* 358, 106–112. <http://dx.doi.org/10.1016/j.quaint.2014.09.077>.
- Yang, T., Wang, C., Chen, Y., Chen, X., Yu, Z., 2015. Climate change and water storage variability over an arid endorheic region. *J. Hydrol.* 529, 330–339. <http://dx.doi.org/10.1016/j.jhydrol.2015.07.051>.
- Yao, T., Thompson, L., Yang, W., Yu, W., Gao, Y., Guo, X., Yang, X., Duan, K., Zhao, H., Xu, B., Pu, J., Lu, A., Xiang, Y., Kattel, D.B., Joswiak, D., 2012. Different glacier status with atmospheric circulations in Tibetan Plateau and surroundings. *Nat. Clim. Change* 2 (9), 663–667. <http://dx.doi.org/10.1038/NCLIMATE1580>.
- Yi, H., Wen, L., 2016. Satellite gravity measurement monitoring terrestrial water storage change and drought in the continental United States. *Sci. Reports* 6, 19909. <http://dx.doi.org/10.1038/srep19909>.
- Yirdaw, S.Z., Snelgrove, K.R., Agboma, C.O., 2008. GRACE satellite observations of terrestrial moisture changes for drought characterization in the Canadian Prairie. *J. Hydrol.* 356 (1–2), 84–92. <http://dx.doi.org/10.1016/j.jhydrol.2008.04.004>.
- Zaitchik, B.F., Rodell, M., Reichle, R.H., 2008. Assimilation of GRACE terrestrial water storage data into a land surface model: results for the Mississippi river basin. *J. Hydrometeorol.* 9 (3), 535–548. <http://dx.doi.org/10.1175/2007JHM951.1>.